PROCEEDINGS, 41st Workshop on Geothermal Reservoir Engineering
Stanford University, Stanford, California, February 22-24, 2016
SGP-TR-209

Modeling Thermal Breakthrough in Sedimentary Geothermal System, Using COMSOL Multiphysics

Kamran Jahan Bakhsh[1], Masami Nakagawa[1], Mahmood Arshad[1], and Lucila Dunnington[1]

[1]Department of Mining Engineering, Colorado School of Mines, Golden, CO, USA

kjahanba@mine.edu , mnakagawa@mines.edu , harshad@mines.edu , ldunning@mines.edu

Keywords: Thermal breakthrough, sedimentary geothermal reservoir, COMSOL, Permeability

ABSTRACT

It is known that premature thermal breakthrough in the production well and cooling due to injection of cold water into a geothermal reservoir can degrade the quality of the reservoir operation. As the heat and mass transfer in the reservoir depends on the internal features of the reservoir and the interfacial features of surrounding rocks, there has been an increased effort to model geothermal reservoirs with detailed pore structures. In this work, the effect of heat extraction on advancement of cold front in both reservoir and surrounding host rock will be discussed. A segment of the deep sedimentary basin consists of high permeable fracture in a region with high temperature gradient is modeled. The influence of variable permeability on heat transfer within reservoir will be numerically investigated. COMSOL Multiphysics is used to generate models with different permeability distribution for host rock.

1. INTORDUCTION

The idea of extracting energy from deep Hot Dry Rock (HDR) where the rock temperature can rise to 350^{o}C at a depth of 5km was proposed four decades ago during the first oil crisis. In 1971, Los Alamos National Laboratory experiment demonstrated the successful utilization of the heat from high temperature deep crystalline rock to generate electricity (Armstead & Tester, 1987). Several projects have since then been conducted to move this concept forward and high temperature crystalline formation became the main target for the geothermal power production.

While prospective areas of crystalline-rock geothermal system is limited to volcanic and tectonically active setting, sedimentary geothermal systems remain largely unexplored, even though they comprise extensive region around the world. Accordingly, the total energy content of sedimentary EGS resources is considerably higher than that of crystalline-rock. For example, the estimated energy content of the U.S. sedimentary rock formation to 10km depth is about 100,000e18 joules (Tester, 2006). The undervalued potential of geothermal from sedimentary rock presents a significant contribution to the future of the world energy portfolio.

Utilization of the heat from sedimentary structures was limited to direct (non-electricity generating) applications for a long time. The Carpathian Basin in Hungary covered 1200 buildings in Szeged (southern Hungary) and greenhouse area about 400,000 m^2 at the end of 1969 (Boldizsar, 1970). More recently, the number of sedimentary based geothermal wells in Hungary has grown to 1,275, all intended for direct applications (Árpási, 2003).

The Guanzhong sedimentary basin in Shaanxi, China (Erlingsson, et al., 2010) provides 3.5 million m^2 of geothermal space heating from 346 geothermal wells as of 2007 (Zhonghe, et al., 2010). Paris and Aquitaine Basin in France (Laplaige, et al., 2005) are other successful direct application examples. Jiachao (2012) reviewed the utilization experience of sedimentary geothermal resources in several locations worldwide and assessed the main characteristics of sedimentary geothermal reservoir particularly at Xianyang and Xiongxing geothermal system in china.

Harvesting energy for power generation from moderately high to medium temperature reservoirs in sedimentary formations was not considered operationally feasible until the development of the binary cycle geothermal power plant, which can utilize lower temperatures geothermal reservoir as low as 120^{o}C. with the binary system, German engineers have successfully generate electricity on a commercial scale, using deep sedimentary formations. Steady electrical power generation of 3.36 MWe from the Bavarian Molasses basin and 3.0 MWe from the Upper Rhine Graben formation exemplifies the promise of the sedimentary geothermal reservoirs (Weber, et al., 2015 & Agemar, et al., 2014).

Sedimentary Enhanced Geothermal System (SEGS), based on the concept of EGS, changes the target area of EGS from crystalline rock to the sedimentary basins. The new focus on sedimentary rock allows for the integration of tried-and-true reservoir stimulation techniques from the oil and gas industry with the frontier of geothermal energy extraction.

Several research papers have been published on different aspects of sedimentary geothermal reservoirs. Gringarten & Sauty (1975) developed an analytical model for predicting thermal breakthrough in a horizontal porous reservoir with uniform thickness. They analytically calculated the optimum distance between wells of doublets system that can keep the temperature of production well as constant as possible. Dogger aquifer near Paris, France has been operated for decades using Gringarten scheme (Alain & Gringarten, 1978-79).

Major sedimentary basins of Colorado such as the Denver Basin, the Piceance Basin and the San Luis Basin have been proposed as candidates for electricity generation in conjunction with direct application (Morgan & Sares, 2011). Morgan (2013) also highlighted the advantages of using a sedimentary basin as an EGS field laboratory to examine aspects of the EGS system.

De Graaf, et al. (2010) reviewed the capability of the Coast Geothermal Project within Australia's hot sedimentary basins to generate large amounts of competitively priced, zero-emission, base-load power. The potential of stratigraphic reservoirs of the Great Basin in the Western U.S to produce heat energy also have been investigated and results showed the possibility of high thermal recovery without need for reservoir enhancement (Allis, et al., 2011).

In Germany, the former gas exploration well, Groß Schönebeck reopened and deepened to access the Lower Permian Rotliegend sedimentary formation. Pairing the extended well with a second well completed in late 2006, a doublet system was constructed in order to generate geothermal electricity (Huenges, et al., 2007).

The possibility of using reservoirs in sedimentary rocks to build EGS in the lower Triassic sedimentary formations of central Poland area has been investigated. Researchers on the polish project modeled the performance of a prospective EGS plants using TOUGH2 code. Adjusting the permeability and volume of the fractured zone, they numerically simulated the net power of an EGS plant (Bujakowski, et al., 2015).

Similarly, tow general classes of sedimentary formation in the Great Basin-a multi-layered and single high permeability layer- have been modeled numerically to investigate the rate of heat extraction. Results showed that lower permeability models have better thermal performance (Deo, et al., 2013).

This paper provides a simple conceptual model to investigate the behavior of the SEGS system. Thermal performance of the SEGS system is assessed based on advancement of the cold front in a reservoir. This study focuses on the influence of the formation permeability as a site-specific characteristic. In particular, the effect of high permeability induced or pre-existing natural fracture on reservoir thermal breakthrough time and geometry of the heat transfer volume are inspected. Numerical simulation has been conducted using commercial software, COMSOL Multiphysics. The following section introduces the proposed conceptual model and the steps of problem formulation. This conceptual model is used as a benchmark for the simulation study and by generating different scenarios the effects of the site-specific characteristic on the reservoir thermal performance is examined in the next section.

2. Conceptual model and Problem Formulation

A segment of the deep sedimentary basin with a high temperature gradient of 0.05 K/m, which contains a high permeable fracture is a benchmark scenario for the simulation study. The reservoir is assumed to be homogenous, with a doublet system- an injection and production well- intersecting the porous domain orthogonally at a depth of 3950 and 3550 m respectively (Figure 1). The injection rate is assumed to be constant and equal to the production rate, 40 l/s, and the temperature of reinjection water is considered 35^{o}C. Distribution of porosity and permeability in the basin is assumed to be uniform, 0.1 and 1e-13 m^2 (100mD) respectively. Non-linearity in density, heat capacity and thermal conductivity of the fracture fluid is allowed and properties of the solid phase are assumed constant. It is also assumed that the thermal equilibrium between fluid and solid was attained instantaneously and the solid phase is incompressible. The study area is restricted to a block with side length of 500 m, and for the sake of simplicity, the gravitational effect is negligible.

$$\Omega_r = \{(x,y,z): 0 < x < 500, 0 < y < 500, -4000 < z < -3500\}$$

$$\Omega_{inj} = \{(x,y,z): 240 < x < 260, \quad 250 - r_{inj} < y < 250 + r_{inj}, -3950 - r_{inj} < z < -3950 + r_{inj}\}$$

$$\Omega_{pro} = \{(x,y,z): 240 < x < 260, \quad 250 - r_{pro} < y < 250 + r_{pro}, -3550 - r_{pro} < z < -3550 + r_{inj}\}$$

$$\partial\Omega_f = \{(y,z): 0 < y < 500, -4000 < z < -3500\}$$

represent the computational domain for the reservoir, injection and production well, and fracture respectively. The numerical model is validated in connection with the Gringarten (1978) analytical model. Accordingly, in order to keep balance between the computational cost and accuracy, spatial and temporal discretization of the numerical simulation for the benchmark model is determined. Keeping equal flow rate for injection and production wells leads to a quick steady-state condition and keeps numerical dispersion low.

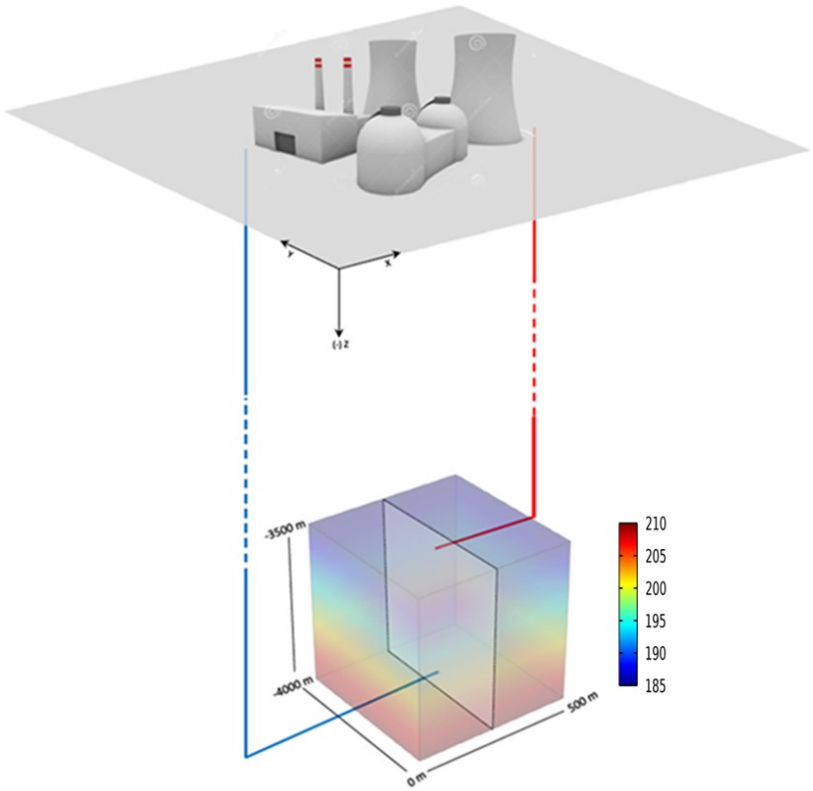

Figure 1: scheme of the conceptual fractured sedimentary basin located in a region with temperature gradient of 0.05 Kelvin per meter

3. GOVERNING EQUATIONS

As the modeled sedimentary basin is assumed to be a homogenous porous media, Darcy's law is used to govern the flow of fluid in the model. Heat transfer governing equations are also derived from energy balance in a domain. One way to model the flow in a fractured reservoir where the flow moves freely through the fractures and relatively slowly within the surrounding porous domain, is to incorporate Darcy's law for the porous media flow in conjunction with Navier-Stokes equation for fracture free-flow. Coupling these two equations and solving them numerically is not cumbersome unless the geometry of the incorporating domains are at different orders-of-magnitude. In this study a very long and narrow fracture domain with high aspect ratio (500×500×0.05) is confined within a very wide porous block of rock (500×500×500). Discretizing the fracture domain explicitly requires a very dense mesh consisting of a huge number of infinitesimally small elements.

An alternative method to avoid an excessive computational cost is a Discrete Fracture Model where the fracture is treated as an interior boundary. The advantage of this approach is in reducing the degrees of freedom (unknowns) and enhancing computational performance particularly for the cases in which the fracture permeability is higher than the surrounding porous medium (Romano-Perez & Diaz-Viera, 2015).

In this study, the permeability of porous domain is considered lower than the fracture permeability for all cases. Accordingly, the discrete Fracture approach is selected for the simulation.

3.1 Fluid flow governing equations

Darcy law is used to govern transient fluid flow in the porous domain.

$$\frac{\partial}{\partial t}(\emptyset_r \rho_r) + \nabla \cdot (\rho_r u) = 0 \qquad x, y, z \in \Omega_r \tag{1}$$

$$u = -\frac{\kappa_r}{\mu} \nabla p \qquad x, y, z \in \Omega_r \tag{2}$$

where, $\emptyset_r$ is the rock matrix porosity (dimensionless), ρ_r is the rock matrix density (kg/m^3), u gives the Darcy's velocity (m/s), κ_r is the rock matrix's permeability (m^2), μ is the fluid dynamic viscosity (Pa.s) and p is the fluid's pressure in the pore (Pa).

The Neumann boundary condition is applied for mass flow at the top and bottom boundaries and the Dirichlet condition is applied for sides of the domain.

$$n \cdot \rho_r u = 0 \quad \text{at } \partial\Omega_r \text{ domain top and bottom facets}$$

where, n is the vector normal to the boundary.

As mentioned above, to avoid high aspect ratio geometry in the model the fracture is considered an interior boundary. Usually at boundaries flow is defined normal instead of tangent to the boundary plane, therefore to govern the velocity field along the fracture, Darcy's law equation must be modified in this boundary condition. This modification is applied to the equation by accounting for fracture thickness.

$$d_f \frac{\partial}{\partial t}(\emptyset_f \rho_f) + \nabla_t \cdot (d_f \rho_f u) = 0 \qquad y, z \in \partial\Omega_f \tag{3}$$

$$u = -\frac{\kappa_f}{\mu} \nabla_t p \qquad y, z \in \partial\Omega_f \tag{4}$$

where, d_f is the fracture's thickness (m), $\emptyset_f$ is the fracture porosity (dimensionless), ρ_f is the fracture density (kg/m^3), u gives the modified Darcy's velocity on the fracture (m/s), κ_f is the permeability of the fracture (m^2), μ is the fluid dynamic viscosity (Pa.s). To restrict the equations to the fracture's plane, ∇_t, the tangential gradient operator is applied for flow in the fracture.

The Neumann boundary condition is applied for mass flow at the fracture edge intersected with the matrix block and hence, no-flow condition is applied on fracture's edges. Constant mass flow rate of 40 l/s is applied at a 20 m of injection and production tube circumference.

$$n \cdot u = 0 \quad \text{at } \partial^2\Omega_f \text{ fracture edges}$$

3.2 Heat transfer governing equations

The following equations are used to govern heat transfer in the porous matrix.

$$(\rho C_p)_{eff} \frac{\partial T}{\partial t} + \rho C_p u \cdot \nabla T + \nabla \cdot q = 0 \tag{5}$$

$$q = -k_{eff} \nabla T \tag{6}$$

$$(\rho C_p)_{eff} = (1 - \emptyset_r)\, \rho_r C_{p_r} + \emptyset_r\, \rho_w C_{p_w} \tag{7}$$

$$k_{eff} = (1 - \emptyset_r)\, k_r + \emptyset_r\, k_w \tag{8}$$

where, $(\rho C_p)_{eff}$ is the effective volumetric heat capacity at constant pressure (J/m3 ^oC), k_{eff}, is the effective thermal conductivity of the rock matrix (J/m s ^oC), and $\rho_w C_{p_w}$, is the volumetric heat capacity of the water . In this study, thermal conductivity of rock matrix is assumed isotropic, hence it is scalar. Second and third terms on the left hand side of the equation represent heat transfer via convection and conduction respectively.

Neumann boundary condition is applied for the heat flow on the top and bottom boundaries. Hence, there is no-heat flux across the top and bottom faces of the rock matrix:

$$-n \cdot q = 0 \text{ at } \partial\Omega_r \text{ rock block facets}$$

Side boundaries of the domain are considered open and the heat can flow in and out of the domain with a specified exterior temperature. The exterior temperature is assumed to be the same as the temperature gradient of the region.

To calculate heat transfer in the fracture, the heat transport equation in a porous matrix needs to be modified to account for the fracture thickness.

$$d_f(\rho C_p)_{eff} \frac{\partial T}{\partial t} + d_f \rho C_p u \cdot \nabla_t T + \nabla_t \cdot q_f = n \cdot q \tag{9}$$

$$q_f = -d_f k_{eff} \nabla_t T \tag{10}$$

$$(\rho C_p)_{eff} = (1 - \emptyset_f)\, \rho_f C_{p_f} + \emptyset_f\, \rho_w C_{p_w} \tag{11}$$

$$k_{eff} = (1 - \emptyset_f)\, k_f + \emptyset_f\, k_w \quad (12)$$

where, $(\rho C_p)_{eff}$ is the effective volumetric heat capacity of the fracture-fluid volume at constant pressure (J/m3 ^oC), k_{eff}, is the effective thermal conductivity of fluid-fracture mixture (J/m s ^oC) . The third term in the left hand side of the equation 9 represents conductive heat flux in the fracture-fluid volume where the computational domain is restricted by the tangential gradient and the term on the right gives the heat supply through the fracture walls by conduction.

Initially, the temperature everywhere in the system is following the defined temperature gradient of the region.

$$T_r(X, Y, Z, 0) = T_f(Y, Z, 0) = T_s - 0.05\, z \qquad x, y, z \in (\Omega_r \cap \partial\Omega_f)$$

where, T_s is the surface temperature (^oK), z is the depth (m), T_r is the porous domain temperature (^oK), and T_f is the fracture domain temperature (^oK).

The Dirichlet boundary condition is applied to fix the temperature of the injection fluid at 35^{o}C.

$$T(X, Y, Z, t) = 35℃ \qquad \text{at } x, y, z \in \text{circumference of the injection well}$$

Parameters used for the benchmark case are summarized in the Table 1. Hydraulic and thermal performance of the reservoir over 30 years of heat extraction is modeled.

Table 1: The benchmark case geometrical parameters and material properties

Parameter		Symbol	Value	Unite
Fracture	aperture	d_f	5	cm
	Length	l	500	m
	Height	h	500	m
	Density	ρ_f	1.2e3	kg/m^3
	Porosity	$\emptyset_f$	0.6	-
	Permeability	κ_f	1e-9	m^2
	Heat capacity	C_{p_f}	1100	J/(kg.K)
	Thermal conductivity	k_f	3	W/(m.K)
Rock matrix	domain length	L	500	m
	Top surface depth	z_T	-3500	m
	Bottom surface depth	z_B	-4000	m
	Density	ρ_r	2587	kg/m^3
	Porosity	$\emptyset_r$	0.1	-
	Permeability	κ_r	1e-13	m^2
	Heat capacity	C_{p_r}	920	J/(kg.K)
	Thermal conductivity	k_r	2	W/(m.K)
Injection and production wells	Borehole radius	r_b	10.8	cm
	Injection length	l_{inj}	20	m
	Production length	l_{pro}	20	m
	Doublet distance	H	400	m
Fracture Fluid (Water)	Dynamic Viscosity	μ	Function of temperature	Pa.s
	Density	ρ_w		kg/m^3
	Heat Capacity	C_{p_w}		J/(kg.K)
	Thermal conductivity	k_w		W/(m.K)
Other	Surface Temperature	T_s	10	deg C
	Geothermal gradient	G	0.05	K/m
	Time period of modeling	a	30	year

4. SIMULATION RESULTS

To analyze the performance of the reservoir, the evolution of the fluid and the temperature fields in the domain of interest over 30 years of reinjection of cold fluid is simulated. As the fluid moves faster through the fractures and relatively slower through the surrounding porous media, the temperature field of the domain follows a similar pattern with the fracture plane becoming cooler than surrounding porous media (Figure 2). A local sharp temperature gradient between fracture plan and surrounding is developed. This gradient combined with the global temperature gradient of the region determines the thermal performance of the reservoir, and their contribution in reservoir thermal performance changes as time elapses.

Figure 3 shows the 179°C iso-temperature surface and its evolution over the course of 30 years of reservoir operation. The volume under 179°C iso-temperature surface is called the "heat transfer area", in which the temperature drop is at least 15% of the maximum value. This volume is affected by a considerable horizontal temperature gradient imposed by cold-water injection. The contrast between these two temperatures gradients is greater near the injection well, resulting in the localized bulging of the iso-temperature surface. As time elapses, the heat transfer area around the line of injection grows faster than the heat transfer area around the production end, forming bell-like shape (Figure 3).

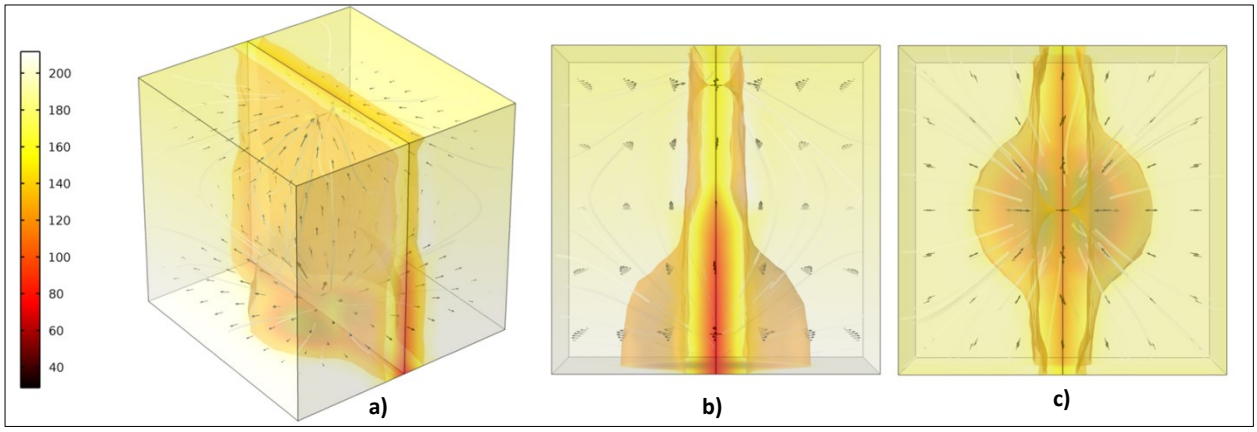

Figure 2: Hydraulic and thermal performance of the benchmark reservoir model over 30 years of heat extraction a) isometric view b) side view c) plan view

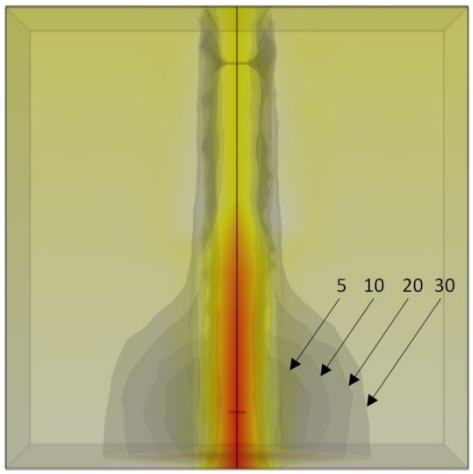

Figure 3: Temperature evolution over 30 years of reservoir operation. Isotemperature surface of 179°C for year 5, 10, 20, and 30 are labeled to demonstrate heat transfer area evolution

The evolving fluid temperature at the production well shows the effect of the high permeability fracture at the time of thermal breakthrough. Figure 4.a shows a sharp decline in the produced fluid temperature at an early stage of the heat extraction due to the relatively low resistance of the fracture to the flow. The slight temperature increase in the first year (expanded in Figure 4.b) is due to the configuration of the doublet system, which the injection well is located below the production well. The lower injection well allows the fluid to access higher temperatures (>185°C) before it migrates toward the higher, cooler production well horizon (185°C).

To illustrate the role of a high permeability fracture in thermal breakthrough time, Figure 4.b shows the production temperature over a logarithmic time scale for a reservoir with and without a fracture, respectively. This results shows that although a high permeability fracture benefits the hydraulic performance of the reservoir, utilizing an optimum reservoir enhancing scheme to balance the hydraulic and thermal performance without early thermal breakthrough in the production well is crucial.

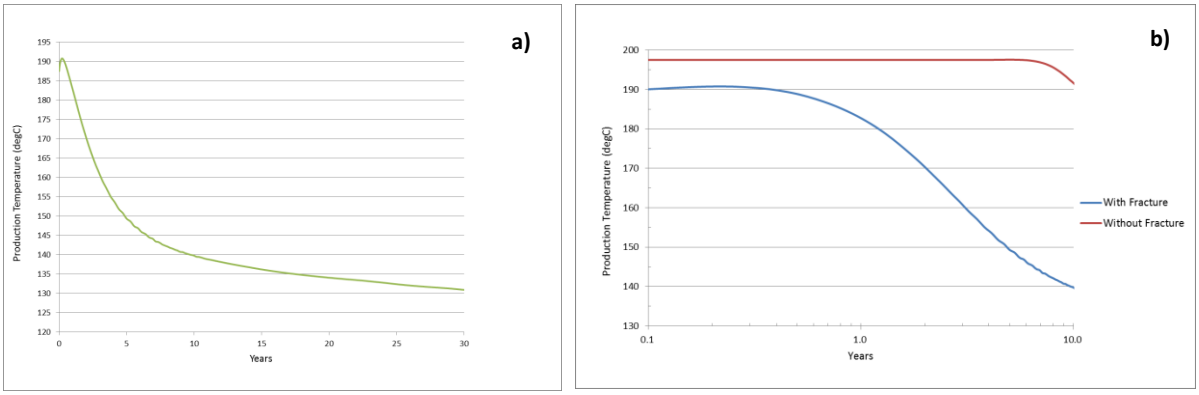

Figure 4: Fluid average temperature verses time: case with high permeability fracture (a) and comparison of production temperature of case with and without high permeability fracture, logarithmic scale (b).

Figure 5.a shows volume of the heat transfer area, normalized by total volume of the domain, versus operation time. The figure can describe the contribution of the reservoir in the thermal performance of the reservoir. It appears that contribution is growing as time is elapsing. However, after 30 years, less than 25% of the domain contributes to heat extraction form the reservoir. This relationship is reasonable, since at an early stage of the injection the majority of the fluid moves freely through the fracture and just a small portion percolate into the surrounding porous domain.

To address the thermal circulation pattern in the basin and to assess its evolution during the 30 years of heat extraction, the average temperature of the fracture surface and the domain boundaries are monitored (Figure 5.b). The graph shows that during the first years of production, longitudinal heat transfer is dominant and after eight years, lateral heat transfer takes over. This behavior might be important in terms of stress regime redistribution in the area, but that is out of scope of this paper.

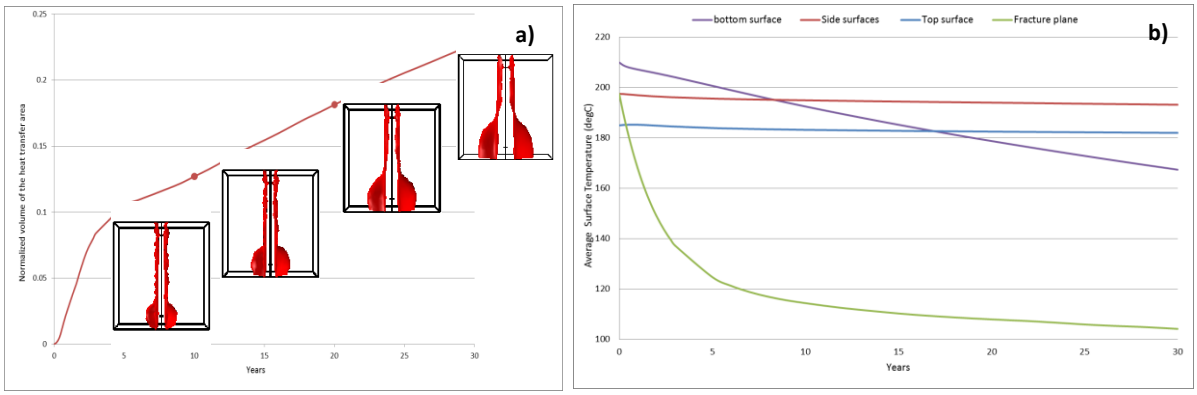

Figure 5: evolution of heat transfer region that contributes in the reservoir thermal performance, normalized valve (a), and average temperature of the domain boundaries over 30 years of heat extraction (b)

4.1 Effect of reservoir permeability on thermal breakthrough time and reservoir thermal performance

Deep sedimentary basins ranging from 2.0 to 6 km with high temperature gradients would be good candidates for generating electricity through SEGS system. To investigate the effect of permeability on the reservoir's thermal performance, different permeabilities are imposed on the fractured reservoir model. 1, 10, 100mD are typical permeabilities applied, and permeability of 500mD was included for the sake of comparison, even though it represent an unrealistic sedimentary structure.

Figure 6.a shows the production temperature over 30 years for the four cases. All curves show a same trend, with permeability having little effect on the thermal breakthrough time. This might be due to the presence of the high permeability fracture, which serves as a bypass for fluid. The average temperature of produced fluid particularly after 5 year, are positively correlated with permeability. The 1mD and 10mD scenarios produced almost the same temperature 5^{o}C lower than benchmark case (100mD). The rare scenario of 500mD permeability produced temperatures about 15^{o}C higher than the benchmark case. The observed outcome is reasonable since the volume of the reservoir contributing its thermal performance is larger when higher permeability allows the fluid more access to the hot rock. Figure 6.b corroborate this explanation, presenting the normalized volume of the heat transfer area versus production years. The growth rate of volume of the heat transfer area is highest in the case of 500mD permeability.

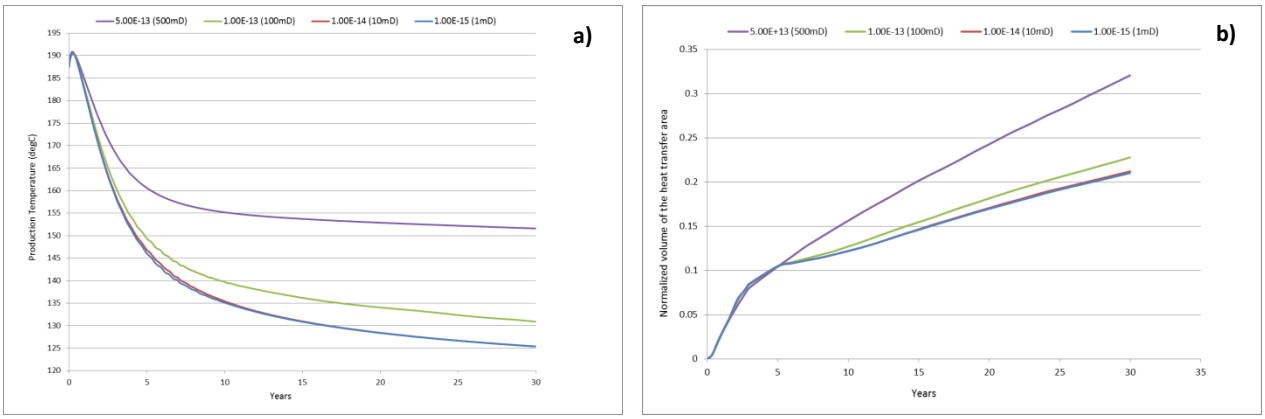

Figure 6: production temperature over 30 years for cases with permeability of 1, 10,100, and 500mD (a) and comparison of the volume of the heat transfer area for cases with different permeability during heat extraction, Normalized valve (b)

4.2 Effect of boundaries on reservoir thermal performance

In this section, the effect of the boundary conditions on reservoir thermal performance is investigated. The same boundary condition has been applied to the benchmark model and all other simulation model. It was assumed that the top and bottom allow no mass and heat flux. The side boundaries were assumed open, so mass and heat can flux through the domain's sides. A model with this configuration can be a good representation of a SEGS for relatively undeformed horizontally stratified beds deposited from a marine environment, which may extend several kilometers laterally but bounded vertically by gradation or clay layers such as in the Midland Basin.

To address the effect of different boundary conditions on the model, two more configurations are studied: a model with open boundaries where heat and mass can flux within the all boundaries, and a model with closed boundaries where the domain is well insulated from surrounding. First model could be representative of a SEGS for rounded, equidimensional, tens of kilometers sedimentary basins such as Intracratonic basins. The second model might be applicable for Lagunal, Fluvial or Estuarine structures in the stratigraphy, surrounded by impermeable beds such as some Pembina Field deposits.

Figure 7 depicts the temperature field in the reservoir at year 30 for the three aforementioned scenarios. Figure 7.a, 7.b, and 7.c show the side view of the temperature field for models with open, confined from top and bottom, and closed boundaries respectively. The plan view of these scenarios is also given in the Figure 7.d, 7.e, and 7.f. The shapes of the heat transfer volume for all three cases are almost the same, except the bottom part of the open boundary case becomes more pear-shaped. In case with open boundaries, fluid, as an energy carrier, has access to more heat than other two cases in which heat cannot come through the boundaries.

Figure 7 also shows that by completely insulating the model the cooling zone (Red colored area) is extended vertically along the fracture plane. This also can be proven by showing produced fluid temperature during heat extraction. Figure 8 shows that the production temperature drops to almost 90^{o}C for the well-insulated case while for the case with open boundaries production temperature only get to 148^{o}C.

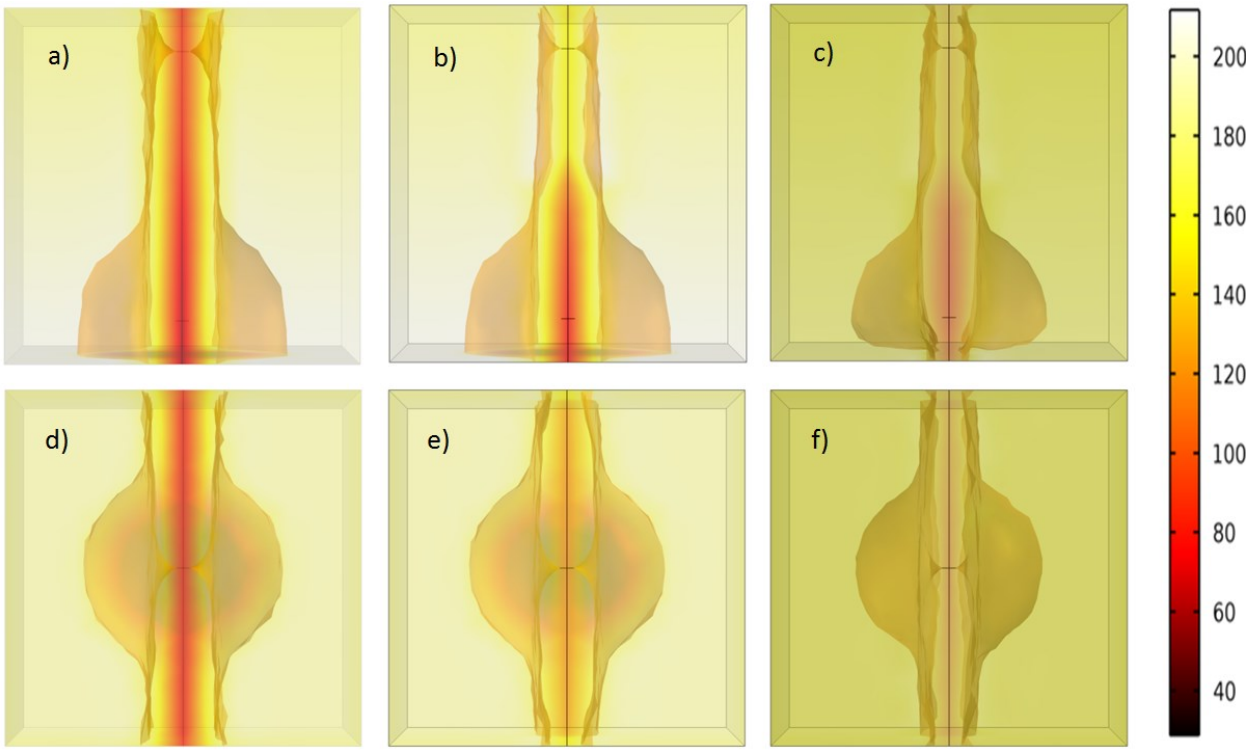

Figure 7: Side view of the temperature field for models with open (a), confined from top and bottom (b), and with closed boundaries (c). Plan view of the models are depicted respectively (d,e, and f)

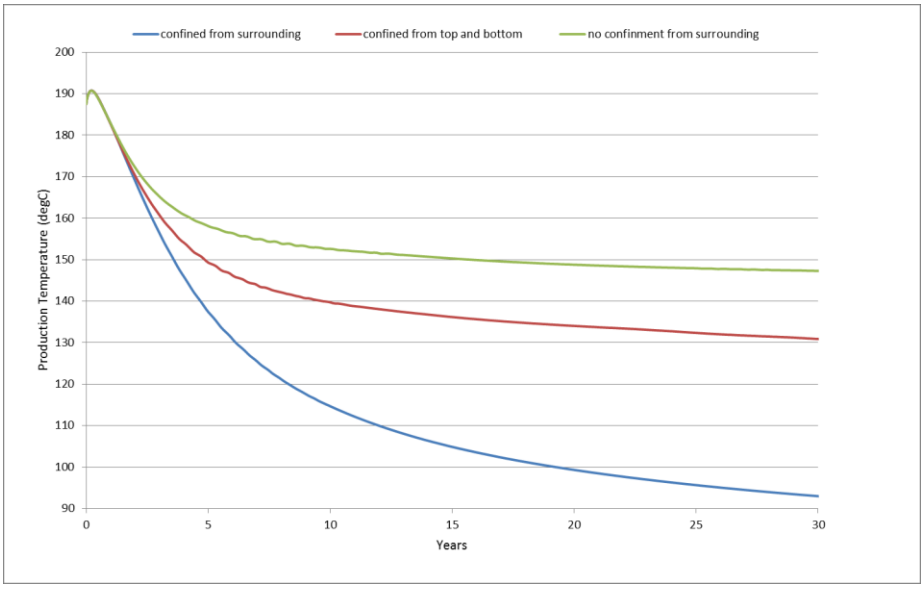

Figure 8: comparison of production temperature for cases with different boundary system: reservoir with well-insulated boundaries from surrounding (blue), with confinement from top and bottom (red) and with no condiment from surrounding (green)

5. CONCLUSION AND DISCUSSION

This study used a simple conceptual model to investigate the behavior of a SEGS system. The model first showed that the presence of induced or pre-existing fractures significantly shortens thermal breakthrough time. The heat transfer area during heat extraction appears as an expanding dome, dictated by the horizontal temperature gradient imposed by cold-water injection through a highly permeable fracture. The results indicate that the volume of the heat transfer area grows faster near the injection point.

Next, a series of permeabilities were applied to the model's host rock. While permeability had no significant effect on thermal breakthrough times since, perhaps, fluid preferentially flowed through the fracture, higher permeability resulted in higher production temperature. Sensitivity of the production temperature to the formation permeability is reduced for the formation with lower permeability. The volume of the heat transfer area reached 32% of the total volume of the domain for a model configuration with highest basin permeability (500mD). This result indicates that even for the case with highest permeability just a portion of the domain contributes in the heat transfer process.

Therefore, multi-stage hydraulic fracturing, which allows access to incrementally bigger volumes of the basin, can be an option to enhances the rock contribution in heat transfer process. However, since over-fracturing may lead to premature thermal breakthrough. It is crucial to balance the hydraulic and thermal performance of the SEGS according to the site-specific characteristics.

Three different boundary systems were imposed on the same reservoir for comparison. Well insulated, confined from top and bottom but open on the sides, and completely open. The evolution of the thermal performance of each scenario showed that the more access the fluid had to heat through domain boundaries (i.e., case with open boundaries) the higher the production temperature. The shape of the heat transfer area also shrunk for the case with open boundaries

Although it is much simplified, the conceptual model used in this study shows that although permeability as an intrinsic feature of the sedimentary formation affects both the hydraulic and thermal performance of the reservoir, presence of high permeability fracture and distinct boundary condition can change the simulation result significantly. The varying results suggest that for successful sedimentary EGS, it is crucial to identify site-specific characteristics of the target basin. Afterwards, compatible reservoir enhancing techniques and suitable models with proper boundary conditions can be employed.

REFERENCES

Agemar, T., Weber, J. & Schulz, . R., 2014. Deep Geothermal Energy Production in Germany. *Energies ,* pp. 4397-4416.

Alain , C. & Gringarten, A. C., 1978-79. Reservoir Lifetime and Heat Recovery Factor in Geothermal Aquifers used for Urban Heating. *pure and applied geophysics ,* Volume 117, pp. 297-308 .

Allis, R., Moore, J., Blackett, B. & Gwynn, M., 2011. *The potential for basin-centered geothermal resources in the Great Basin.* San Diego, CA, Geothermal Resources Council Annual Meeting .

Armstead , H. & Tester, J., 1987. *Heat mining.* New Fetter Lane, London: E. & F. N. Spon Ltd.

Árpási, M., 2003. Geothermal development in Hungary—country update report 2000–2002. *Geothermics,* p. 371–377.

Boldizsar, T., 1970. Geothermal Energy Production from Porous Sediments in Hungary. *Geothermics,* Volume 2.

Bujakowski, W. et al., 2015. Modelling geothermal and operating parameters of EGS installations in the lower triassic sedimentary formations of the central Poland area. *Renewable Energy ,* Volume 80, p. 441e453.

de Graaf, L., Palmer, R. & Reid, I., 2010. *The Limestone Coast Geothermal Project, South Australia: a Unique Hot Sedimentary Aquifer Development.* Bali, Indonesia, Proceedings World Geothermal Congress .

Deo, M., Roehner, . R., Allis, . R. & Moore, J., 2013. *Reservoir Modeling of Geothermal Energy Prpduction From Stratigraphic Reservoirs in The Great Basin.* Stanford University, Stanford, California, Thirty-Eighth Workshop on Geothermal Reservoir Engineering.

Erlingsson, T., Jóhannesson, T., Olafsson, E. & Axelsson, G., 2010. *Geothermal District Heating System in XianYang, Shaanxi, China.* Bali, Indonesia, Proceedings World Geothermal Congress .

Gringarten, A. C. & Sauty, J. P., 1975. A theoretical Study of Heat Extraction From Aquafires with Uniform Regional Flow. *Journal of Geophysical Research,* 80(35).

Huenges, E. et al., 2007. *Current state of the EGS project Groß Schönebeck – drilling into the deep sedimentary geothermal reservoir.* Unterhaching, Germany, Proceedings European Geothermal Congress.

Jiachao, H., 2012. *Assessment and management of sedimentary geothermal resources, Master's thesis,* Iceland: School of Engineering and Natural Sciences,University of Iceland.

Laplaige, P. et al., 2005. *Geothermal Resources in France - Current Situation and Prospects.* Antalya, Turkey, Proceedings World Geothermal Congress .

Morgan, P., 2013. *Advantages of Choosing a Sedimentary Basin as the Site for an EGS Field Laboratory.* Las Vegas, Geothermal Resource Council.

Morgan, P. & Sares, M. A., 2011. *New Horizons for Geothermal Energy in Sedimentary Basins in Colorado.* s.l., Geothermal Resources Council.

Romano-Perez, C. A. & Diaz-Viera, M. A., 2015. *A Comparison of Discrete Fracture Models for Single Phase Flow in.* Boston, COMSOL Conference.

Tester, J. e. a., 2006. *The future of geothermal energy - Impact of Enhanced Geothermal systems (EGS) on the US in the 21st,* Idaho Falls, Idaho.: Idaho National Laboratory.

Weber, J. et al., 2015 . *Geothermal Energy Use in Germany.* Melbourne, Australia, Proceedings World Geothermal Congress .

Zhonghe, P., Fengtian, Y., Tianming, H. & Zhongfeng , D., 2010. *Genesis Analysis of Geothermal Systems in Guanzhong Basin of China with Implications on Sustainable Geothermal Resources Development.* Bali, Indonesia, Proceedings World Geothermal Congress.